

PROCEDURAL MISTAKE DETECTION VIA ACTION EFFECT MODELING

Wenliang Guo, Yujiang Pu, Yu Kong

Department of Computer Science and Engineering
Michigan State University
East Lansing, MI 48824, USA
{guowenli, puyujian, yukong}@msu.edu

ABSTRACT

Mistake detection in procedural tasks is essential for building intelligent systems that support learning and task execution. Existing approaches primarily analyze how an action is performed, while overlooking what it produces, i.e., the **action effect**. Yet many errors manifest not in the execution itself but in the resulting outcome, such as an unintended object state or incorrect spatial arrangement. To address this gap, we propose Action Effect Modeling (AEM), a unified framework that jointly captures action execution and its outcomes through a probabilistic formulation. AEM first identifies the outcome of an action by selecting the most informative effect frame based on semantic relevance and visual quality. It then extracts complementary cues from visual grounding and symbolic scene graphs, aligning them in a shared latent space to form robust effect-aware representations. To detect mistakes, we further design a prompt-based detector that incorporates task-specific prompts and aligns each action segment with its intended execution semantics. Our approach achieves state-of-the-art performance on the EgoPER and CaptainCook4D benchmarks under the challenging one-class classification (OCC) setting. These results demonstrate that modeling both execution and outcome yields more reliable mistake detection, and highlight the potential of effect-aware representations to benefit a broader range of downstream applications.

1 INTRODUCTION

Mistakes are inevitable in procedural tasks, from cooking and assembly to medical procedures. While humans refine their skills through learning and experience, they often overlook subtle execution details that lead to unintended outcomes. For instance, a person might follow what seems to be the correct cutting motion, yet still produce irregular cucumber slices due to a slight misalignment in technique. These errors may not be immediately apparent from the action itself but become evident in the final result. To better support users in performing tasks, intelligent systems must therefore assess not only how actions are performed, but also what those actions ultimately produce.

Existing mistake detection approaches focus primarily on modeling the execution process, assessing correctness by analyzing motion patterns and action sequences. Previous works have explored such methods in structured tasks, such as assembly (Sener et al., 2022) and cooking (Wang et al., 2023; Peddi et al., 2023), often relying on frame-level classification or multimodal features. More recently, Lee et al. (2024) introduced prototype learning to evaluate execution similarity across instances, while Huang et al. (2025a) utilized task graphs to predict all possible next actions and compared them with actual executions in the latent space. However, a shared limitation of these methods is the assumption that mistakes can be identified solely from the execution process, without verifying whether the final outcome aligns with the intended result.

In real-world scenarios, the execution may appear correct, yet minor deviations can lead to flawed outcomes. As illustrated in Figure 1a, an imprecise stirring position might resemble a correct motion, while the resulting spillage reveals the error. In Figure 1b, subtle differences in slicing technique may produce irregularly shaped slices. These examples underscore a critical limitation: mistake detection should account for not only the execution process but also the resulting action effect.

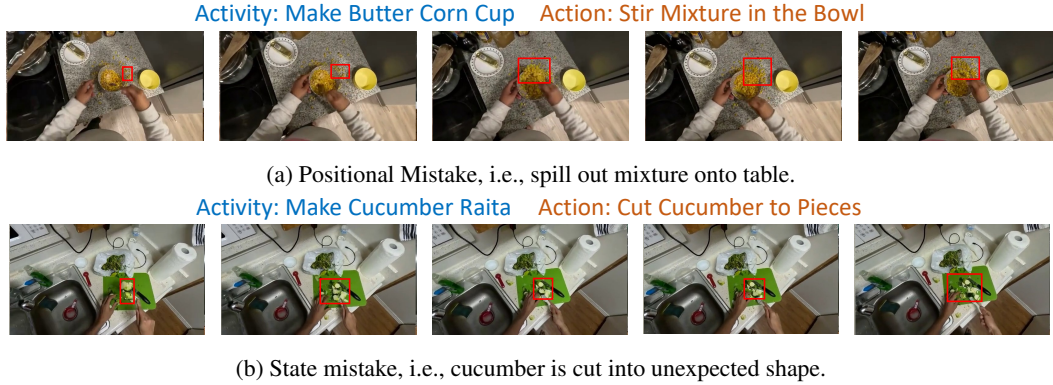


Figure 1: Examples of two types of mistakes: object positional and state mistakes, in cooking scenario from CaptainCook4D dataset (Peddi et al., 2023).

We address this challenge by casting mistake detection as a marginalization problem over latent variables including potential action effects. Concretely, the probability of a mistake is modeled as a joint function of both the execution of an action and its outcome. This probabilistic view naturally decomposes the task into three subproblems: identifying the action effect, interpreting the effect, and determining whether it reveals a mistake. Based on this formulation, we propose **Action Effect Modeling (AEM)**, a unified framework that enriches action representations with effect-aware features. AEM first selects an effect frame that best reflects the result based on both semantic relevance and visual quality. The action effect is then modeled from two complementary perspectives: *object states*, which capture visual attributes such as shape and size changes, and *spatial relationships*, which describe how objects are arranged relative to one another.

To learn robust and interpretable effect-aware representations, AEM leverages multimodal supervision from vision-language models (Hurst et al., 2024) through dual branches. The visual branch encodes grounded object features and positions, while a textual branch constructs symbolic scene graphs to extract attributes and relational descriptions. During training, these supervision signals are aligned in a shared latent space via contrastive objectives, allowing the model to distill structured effect knowledge into a compact representation. At test time, the learned effect representation is fused with the action segment features, providing enriched context for downstream mistake detection.

While action effects provide valuable cues, effective mistake detection also requires modeling the execution itself. To this end, we develop a prompt-based detector that evaluates whether an action segment aligns with its execution process within the task context. Rather than relying on frame-level classifiers, our detector encodes each action using a learnable representation and aligns it with a task-specific textual prompt in a contrastive manner. By modeling both the temporal dynamics and the resulting effect of an action, the model captures rich semantic cues to distinguish subtle execution errors as well as outcome discrepancies. Our approach is evaluated on two challenging egocentric datasets, EgoPER (Lee et al., 2024) and CaptainCook4D (Peddi et al., 2023), achieving state-of-the-art performance. Extensive ablations further demonstrate the necessity and effectiveness of action effect modeling in improving mistake detection.

In summary, our contributions are threefold:

- We formulate mistake detection as a probabilistic marginalization over latent action effects, decomposing the task into effect frame sampling, effect modeling, and mistake classification.
- We propose Action Effect Modeling to learn effect-aware action representations by capturing object state and spatial relationships using complementary visual and symbolic cues.
- We develop a prompt-based detector that aligns action segments with task-specific textual prompts, enabling effective detection of both execution errors and outcome errors in context.

2 RELATED WORK

Mistake Detection consists of two main branches: online detection (Jang et al., 2019; Ding et al., 2023; Narasimhan et al., 2023; Ashutosh et al., 2024; Flaborea et al., 2024; Plini et al., 2024; Soran

et al., 2015; Jang et al., 2023) and offline detection (Sener et al., 2022; Wang et al., 2023; Haneji et al., 2024; Peddi et al., 2023; Schoonbeek et al., 2024; Ghoddoosian et al., 2023; Lee et al., 2024; Mazzamuto et al., 2024; Storks et al., 2024; Huang et al., 2025a). Online mistake detection focuses on detecting sequential mistakes in real time, while offline detection aims to recognize incorrect action execution. This work primarily addresses offline mistake detection.

Zooming into the offline detection, early approaches relied on training binary classifiers with visual or multimodal inputs (e.g., text, audio, depth) to learn implicit action representations, without explicitly modeling the underlying action dynamics (Sener et al., 2022; Haneji et al., 2024; Peddi et al., 2023). More recently, Lee et al. (2024) introduced a prototype-based method that explicitly models actions by clustering features during training to learn representative action embeddings. Huang et al. (2025a) utilized task graphs to predict possible next steps and reconstructed action feature in the latent space. Both methods realized error detection through similarity comparison between predicted and input action features at inference time.

While these methods achieve strong performance, they predominantly focus on modeling the execution process. However, the inherent variability of human behavior poses a significant challenge for detecting fine-grained mistakes solely from execution dynamics. This limitation motivates us to go beyond modeling the action itself by incorporating action effects as complementary signals, thereby enhancing the robustness and reliability of mistake detection.

Video Anomaly Detection (Wu et al., 2019; Gong et al., 2019; Pu & Wu, 2022; Wu et al., 2022; Al-Lahham et al., 2024; Pu et al., 2024) is closely related to mistake detection, where models are typically trained on normal videos and identify anomalies as statistical deviations, without requiring prior knowledge of specific abnormal events. However, mistake detection in procedural videos is inherently goal-oriented, as it requires an understanding of structured workflows to assess whether an action is executed correctly. In addition, VAD is predominantly used in surveillance systems, where the camera view remains fixed and the dynamics of the scene is relatively stable. In contrast, procedural videos, especially in egocentric views, involve more fine-grained human activities, explicit scene transitions, and dynamic human motion, making action-effect modeling more challenging but crucial for building life assistive system.

3 METHODOLOGY

3.1 PROBLEM FORMULATION.

Given a procedural video corresponding to a predefined task, our goal is to determine whether each segmented action is executed correctly or contains a mistake. We operate on non-overlapping segments, where each segment is denoted as a tuple $s = (t_s, t_e, a, y)$, with t_s and t_e denoting the start and end timestamps, a the action label, and $y \in \{0, 1\}$ the binary mistake label ($y = 1$ indicates a mistake). Following the one-class classification (OCC) setting (Lee et al., 2024; Huang et al., 2025a), the training set includes only normal actions ($y = 0$), while the test set contains both correct and erroneous segments.

Formally, the objective is to estimate the probability of a mistake given a visual representation of the segment, expressed as $P(\hat{y} \mid \mathbf{X})$, where \mathbf{X} denotes the encoded segment feature and \hat{y} is the predicted mistake label. Unlike prior methods that classify segments solely based on execution dynamics, we argue that procedural correctness depends on both the execution process and its outcome. This motivates a probabilistic formulation in which mistake detection is expressed as a marginalization over effect frames and the latent effect descriptors:

$$\sum_{i=1}^K \sum_{f_e} \underbrace{P(\hat{y} \mid \mathbf{X}, e_i)}_{\text{mistake detection}} \cdot \underbrace{P(e_i \mid f_e, \mathbf{X})}_{\text{effect-aware learning}} \cdot \underbrace{P(f_e \mid \mathbf{X})}_{\text{frame sampling}}, \quad (1)$$

where f_e denotes the discrete effect frame sampled from the video, and e_i represents the i -th possible descriptor of the action effect extracted from f_e . K is the total number of effect descriptors, which in our case includes two complementary perspectives: object states and spatial relationships, as they reveal common mistakes in procedural activities. Here we assume that once the segment feature \mathbf{X} and the effect descriptor e_i are obtained, the specific effect frame f_e does not provide additional

information for mistake prediction, i.e., $\hat{y} \perp f_e \mid (\mathbf{X}, e_i)$, and $P(\hat{y} \mid \mathbf{X}, e_i, f_e) = P(\hat{y} \mid \mathbf{X}, e_i)$. Intuitively, Eq. 1 indicates that we consider every possible effect frame and each of its associated action-effect descriptors, estimate the likelihood of each (f_e, e_i) combination, evaluate whether it suggests a mistake, and then aggregate these weighted probabilities to obtain the final prediction.

This formulation provides a structured view of mistake detection pipeline: frame sampling, effect-aware learning, and mistake classification, bridging the gap between how an action is performed and what outcomes it produces. Next, we will build a framework following this formulation.

3.2 FRAMEWORK OVERVIEW.

Figure 2 illustrates the overall framework. We first adopt an action segmentation backbone to obtain frame-wise features and non-overlapping action segments. The frame features are concatenated along the temporal dimension based on segment boundaries. The resulting segment features \mathbf{X} are fed into the Action Effect Modeling (AEM) module which (i) performs effect frame sampling $P(f_e \mid \mathbf{X})$ to identify the frame most indicative of the outcome, (ii) extracts multimodal effect knowledge $P(e \mid f_e, \mathbf{X})$ including object states and spatial relationships, and (iii) learns an effect-aware representation aligned across visual and symbolic cues. Finally, the enriched segment features are passed into the mistake detection module, which models $P(\hat{y} \mid \mathbf{X}, e)$ using a prompt-based detector. In the following, we detail three core components: action segmentation, effect modeling and mistake detection.

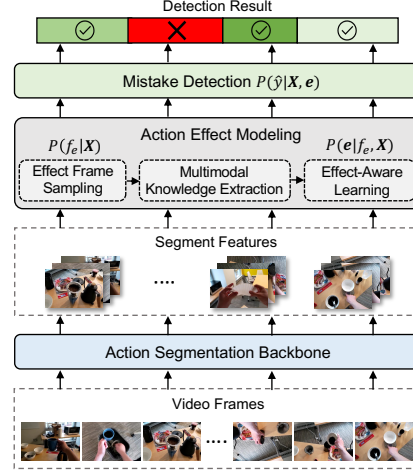


Figure 2: Framework overview.

3.3 ACTION SEGMENTATION

Following Lee et al. (2024) and Huang et al. (2025a), we adopt ActionFormer (Zhang et al., 2022) as the action segmentation backbone, which outputs a feature pyramid with multi-scale temporal resolutions. Inspired by prior work (Yang et al., 2024; Meng et al., 2020), we design a dynamic fusion module to refine temporal representations by adaptively aggregating the multi-scale features from the backbone, while preserving the hierarchical pyramid structure for segment boundary regression. This design aims to provide more discriminative segment features \mathbf{X} for subsequent action effect modeling and mistake detection. Please refer to Appendix ?? for details about this module.

3.4 ACTION EFFECT MODELING

While the segment feature encodes the temporal dynamics of action execution, it is insufficient to capture the subtle yet critical cues manifested in the action’s outcome. To bridge this gap, AEM integrates action effects by extracting multimodal features from selected effect frames and using them as external supervision. These features guide a learnable *effect token*, which distills outcome semantics into the action representation. As illustrated in Figure 3, the entire AEM pipeline consists of three steps: effect frame sampling, multimodal knowledge extraction, and effect-aware learning. It produces enriched effect-aware action representations that capture both execution and outcome.

Effect Frame Sampling. To identify the frame that best captures the outcome of a given action, we rank candidate frames within each action segment based on semantic relevance and visual clarity. For semantic relevance, motivated by Niu et al. (2024), we use GPT-4o (Hurst et al., 2024) to generate textual descriptions of the anticipated post-action states. Then we compute the frame-wise similarity between the segment’s visual feature \mathbf{X} and the description embeddings obtained from a pre-trained text encoder, followed by softmax normalization. For visual clarity, we apply the Laplacian operator to estimate the sharpness of each frame within the segment and normalize the scores between the 5th and 95th percentiles. The final ranking score combines both semantic relevance and visual clarity, and the top-ranked frame is selected as the effect frame.

Multimodal Knowledge Extraction. From the selected effect frame, we extract cues capturing both object states and spatial configurations, as they can reveal errors that occur in most procedural

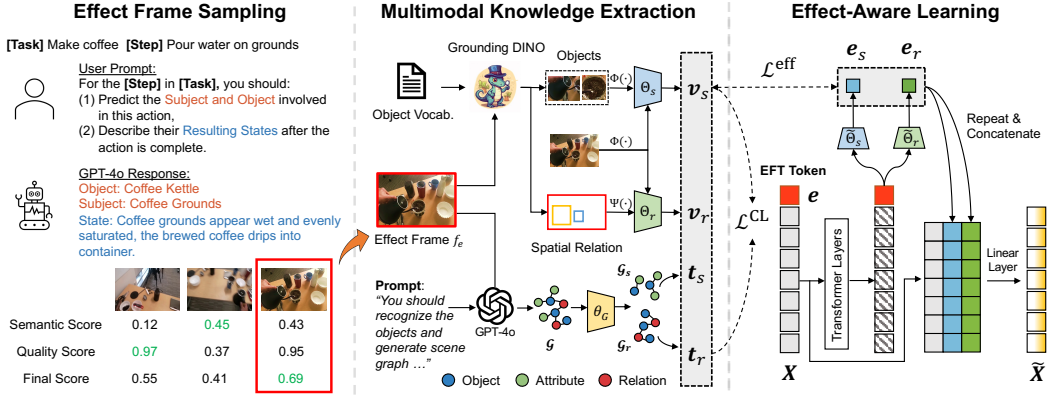


Figure 3: Overview of the Action Effect Modeling (AEM) module. Effect frame sampling and multimodal knowledge extraction are only used to learn effect state and relation projectors Θ_s, Θ_r during training. Both of them are skipped during testing.

activities. We adopt a dual-branch strategy: a visual branch for grounded object-centric features, and a textual branch for symbolic scene abstraction.

In the visual branch, we use Grounding DINO (Liu et al., 2024) to detect relevant objects, then we extract object state and relation features v_s, v_r by concatenating and projecting embeddings:

$$v_s = \Theta_s \left(\Phi(f_e) \parallel (\Phi(f_e^{o_i}))_{i=1}^N \right), \quad v_r = \Theta_r \left(\Phi(f_e) \parallel (\Psi(p_e^{o_i}))_{i=1}^N \right), \quad (2)$$

where f_e is the effect frame, $f_e^{o_i}$ is the cropped i -th object regions, and $p_e^{o_i}$ is the corresponding coordinates of the object bounding boxes. $\Phi(\cdot)$ is a pre-trained image encoder, $\Psi(\cdot)$ is a positional encoding layer, and Θ_s, Θ_r are two different multilayer perceptrons (MLPs). \parallel denotes channel-wise concatenation, and $(\cdot)_{i=1}^N$ represents the successive concatenation of multiple embeddings.

Although visual grounding provides object-centric features that capture appearance and spatial cues from the effect frame, it lacks high-level semantic abstraction and relational reasoning. To address this, we introduce a textual scene graph branch to model the symbolic structure of the action effect. Given an effect frame and objects detected by Grounding DINO, we leverage the recognition and reasoning capabilities of a Multimodal Large Language Model (MLLM) by prompting GPT-4o to generate a scene graph $\mathcal{G} = (\mathcal{V}, \mathcal{E})$, where \mathcal{V} contains three types of nodes: *object*, *relation*, and *attribute*, and \mathcal{E} represents the set of directed edges. We encode the textual labels of all nodes in \mathcal{V} using a pre-trained text encoder to obtain node embeddings, which are then fed into a Graph Neural Network (GNN) (Veličković et al., 2017) to compute context-aware features t_v for each node.

To abstract finer-grained effect information from text modality, we propose to decompose the generated scene graph \mathcal{G} into two disentangled subgraphs: a state subgraph $\mathcal{G}_s = (\mathcal{V}_s, \mathcal{E}_s)$ and a relation subgraph $\mathcal{G}_r = (\mathcal{V}_r, \mathcal{E}_r)$. Specifically, the state subgraph includes the object nodes along with their adjacent attribute nodes, capturing object-level changes such as color or texture. The relation subgraph consists of the same object nodes and the intermediate relation node connecting them, representing spatial relationships such as “above” or “inside.” Given t_v as the GNN feature of each node, we compute the textual features for object states and spatial relations by applying the following average pooling over subgraphs, where $|\mathcal{V}_s|$ and $|\mathcal{V}_r|$ are the number of nodes in each subgraph:

$$t_s = \frac{\sum_{v \in \mathcal{V}_s} t_v}{|\mathcal{V}_s|}, \quad t_r = \frac{\sum_{v \in \mathcal{V}_r} t_v}{|\mathcal{V}_r|}, \quad (3)$$

Effect-Aware Learning. After acquiring multimodal effect features, a central challenge is how to effectively integrate these features into the action representation. A naive approach is to concatenate the effect and action segment features, but this would require querying MLLMs during inference, introducing prohibitive computational overhead. To circumvent this, we treat the effect features as supervision signals and employ a distillation-inspired strategy. Specifically, we introduce a learnable effect token that implicitly captures task-specific action effects through self-attention. During

training, this token is aligned with the multimodal effect features to distill external knowledge into a compact representation. Crucially, at inference time the framework relies only on the learned token, eliminating any dependency on external models to ensure efficient deployment.

As shown in Figure 3, we append the learnable effect token \mathbf{e} to the segment-level features, which are then fed into Transformer encoding layers for temporal modeling. Subsequently, we align the projected effect tokens with the multimodal effect features in the state and relation latent spaces, respectively, which is formulated as:

$$\begin{aligned}\mathcal{L}_s^{\text{eff}} &= \|\tilde{\Theta}_s(\mathbf{e}) - \mathbf{v}_s\|^2 + \|\tilde{\Theta}_s(\mathbf{e}) - \mathbf{t}_s\|^2, \\ \mathcal{L}_r^{\text{eff}} &= \|\tilde{\Theta}_r(\mathbf{e}) - \mathbf{v}_r\|^2 + \|\tilde{\Theta}_r(\mathbf{e}) - \mathbf{t}_r\|^2,\end{aligned}\quad (4)$$

where $\tilde{\Theta}_s(\cdot)$ and $\tilde{\Theta}_r(\cdot)$ are spatial and relation projection layers, respectively. This enables efficient learning of a compact and generalizable effect-aware representation without relying on expensive effect-frame computation by MLLMs during inference time.

To enhance the consistency between the two supervision signals, we introduce a contrastive objective that explicitly aligns their visual and textual representations. While the effect loss encourages the learnable token to match each modality individually, this objective ensures that both modalities encode the same underlying semantics from complementary perspectives. Taking the object state as an example, we treat the visual and textual features $(\mathbf{v}_s, \mathbf{t}_s)$ as positive pairs, and all other samples in the batch as negatives. The contrastive loss is formulated as:

$$\mathcal{L}_s^{\text{CL}} = \sum_i \left[-\log \frac{\exp(\cos(\mathbf{v}_s^i, \mathbf{t}_s^i)/\rho)}{\sum_j \exp(\cos(\mathbf{v}_s^i, \mathbf{t}_s^j)/\rho)} \right], \quad (5)$$

where i and j index samples in the batch, $\cos(\cdot)$ denotes the cosine similarity, and ρ is a temperature coefficient. Similarly, we can calculate the relation contrastive loss as $\mathcal{L}_r^{\text{CL}}$. Together, these objectives enable the effect token to learn a compact multimodal representation of action effects, which is further integrated into the segment features as:

$$\tilde{\mathbf{X}} = \mathcal{F}(\mathbf{X} \parallel \tilde{\Theta}_s(\mathbf{e}) \parallel \tilde{\Theta}_r(\mathbf{e})) \quad (6)$$

where \parallel denotes channel-wise concatenation and $\mathcal{F}(\cdot)$ is a linear projection layer. The resulting fused segment features serve as a strong signal for downstream mistake detection.

3.5 MISTAKE DETECTION

Following previous work (Lee et al., 2024; Huang et al., 2025a), we adopt an one-class classification (OCC) setting for mistake detection, which learns canonical action patterns from correct samples only. Given the effect-enhanced segment features, we first perform an average-pooling over the enhanced effect-aware segment feature $\tilde{\mathbf{X}}$ across temporal dimension to obtain the action embedding \mathbf{x}_a . Instead of learning a binary classifier, we introduce a prompt-based detector to increase task-specific discriminability. For each action label a , we construct a template-based textual prompt \mathcal{P}_a (e.g., “An image showing [ACTION] for [TASK]”), and obtain its representation by:

$$\mathbf{y}_a = E(\mathbf{p} \parallel \text{Embed}(\text{Tokenize}(\mathcal{P}_a))), \quad (7)$$

where \mathbf{p} is a learnable prefix embedding and $E(\cdot)$ is the frozen text encoder. \parallel denotes concatenation.

During training, we align the action embedding with its corresponding prompt features while repulsing it from other prompt embeddings through a contrastive objective:

$$\mathcal{L}^{\text{det}} = -\frac{1}{B} \sum_{i=1}^B \log \left(\frac{\exp(\cos(\mathbf{x}_a^i, \mathbf{y}_a^i)/\rho)}{\sum_{c=1}^C \exp(\cos(\mathbf{x}_a^i, \mathbf{y}_a^c)/\rho)} \right), \quad (8)$$

where \mathbf{x}_a^i denotes the i -th action embedding in a mini-batch B , and C is the total number of actions in a specific task. During inference, we compute the similarity score $\text{sim}(\mathbf{x}_a, \mathbf{y}_a)$ between the action embedding and its corresponding textual prompt by $\text{sim}(\mathbf{x}_a, \mathbf{y}_a) = \cos(\mathbf{x}_a, \mathbf{y}_a)/\rho$. The final prediction of mistake probability can be obtained by $P(\hat{y} \mid \mathbf{X}, \mathbf{e}) = 1 - \text{sim}(\mathbf{x}_a, \mathbf{y}_a)$. The mistake detection result is determined by thresholding the mistake probability:

$$\hat{y} = \begin{cases} 1, & P(\hat{y} \mid \mathbf{X}, \mathbf{e}) > \tau, \\ 0, & \text{otherwise.} \end{cases} \quad (9)$$

where \hat{y} is the predicted mistake label and τ is a predefined threshold.

Table 1: Mistake detection results on the EgoPER dataset (Lee et al., 2024). AUC and EDA are in percentage (%). Best results are **bold**, and second-best are underlined.

Method	Quesadilla		Oatmeal		Pinwheel		Coffee		Tea		All	
	AUC	EDA	AUC	EDA	AUC	EDA	AUC	EDA	AUC	EDA	AUC	EDA
Random	50.0	19.9	50.0	11.8	50.0	15.7	50.0	8.2	50.0	17.0	50.0	14.5
HF ² -VAD	62.6	34.5	62.3	25.4	52.7	29.1	59.6	10.0	62.1	36.6	59.9	27.1
HF ² -VAD + SSPCAB	60.9	30.4	61.9	25.3	51.7	33.9	60.1	10.0	63.2	35.4	59.6	27.0
S3R	51.8	52.6	61.6	47.8	52.4	50.5	51.0	16.3	57.9	47.8	54.9	43.0
EgoPED	65.6	<u>62.7</u>	65.1	51.4	55.0	59.6	58.3	55.3	<u>66.0</u>	56.0	62.0	57.0
AMNAR	<u>71.9</u>	61.4	<u>75.4</u>	<u>65.0</u>	<u>65.4</u>	65.0	<u>67.8</u>	73.5	61.9	<u>57.0</u>	<u>68.5</u>	<u>64.4</u>
Ours	80.8	68.1	77.0	68.6	69.9	<u>61.2</u>	70.3	<u>66.4</u>	71.1	69.4	73.8	66.7

Table 2: Mistake detection results on the CaptainCook4D dataset (Peddi et al., 2023).

Method	Precision	AUC	EDA
Random	44.9	51.2	49.7
EgoPED	56.5	54.9	69.8
AMNAR	<u>66.8</u>	<u>60.2</u>	72.3
Ours	68.1	62.5	<u>71.9</u>

3.6 TRAINING OBJECTIVE

Finally, we jointly optimize three objectives to train the model in an end-to-end fashion: the segmentation loss \mathcal{L}^{seg} following Zhang et al. (2022), the action-effect modeling loss \mathcal{L}^{eff} and \mathcal{L}^{CL} , and the mistake detection loss \mathcal{L}^{det} . The overall training objective is defined as:

$$\mathcal{L} = \mathcal{L}^{\text{seg}} + \mathcal{L}^{\text{eff}} + \mathcal{L}^{\text{CL}} + \mathcal{L}^{\text{det}}, \quad (10)$$

where \mathcal{L}^{eff} and \mathcal{L}^{CL} comprise both state and relation terms. By incorporating action-effect modeling into the training process, our framework learns to attend to semantically meaningful object state transitions and spatial relationships, thereby enhancing both representation and mistake detection.

4 EXPERIMENTS

4.1 EXPERIMENTAL SETUP

Mistake Datasets. We evaluate our method on two egocentric video datasets: EgoPER (Lee et al., 2024) and CaptainCook4D (Huang et al., 2025a). The EgoPER dataset consists of 385 egocentric cooking videos spanning 5 recipe categories, with a total duration of 28 hours. Among these, 213 videos contain only correct actions, while the remaining 178 include various execution mistakes. Following Lee et al. (2024), we use 80% of the normal videos for training, 10% for validation, and the remaining 10% together with all erroneous videos for testing. The CaptainCook4D dataset contains 384 videos covering 24 recipes, with a total length of 94.5 hours. Among all recordings, 164 are labeled as normal, while the remaining 220 videos include incorrect action steps. Following Huang et al. (2025a), we use all normal recordings for training and the erroneous ones for testing.

Evaluation Metrics. We follow prior work (Lee et al., 2024; Huang et al., 2025a) by using Area Under the Curve (AUC) and Error Detection Accuracy (EDA) to jointly measure model’s ability to distinguish correct and erroneous actions within each video. AUC assesses frame-level discrimination between errors and non-errors, whereas EDA measures segment-level detection accuracy. Both metrics are computed by aggregating detection results across a densely sampled threshold range from 0 to 1, rather than relying on a single fixed threshold, enabling a more comprehensive evaluation of the model’s behavior across the full spectrum of thresholds.

Implementation Details. We use off-the-shelf EVA-02 CLIP (Fang et al., 2024) for all the image and text encoding. For the EgoPER dataset, we follow Lee et al. (2024) to use additional features based on Active Object Detection (AOD). For effect frame sampling, the final score is an average of the semantic relevance and visual quality scores. Following Lee et al. (2024) and Huang et al. (2025a), we independently train and test the model in each recipe and report the average of all

Table 3: Ablation studies (a–d), action segmentation results (e), and performance comparison with different scene graph generation models (f) on EgoPER dataset (Lee et al., 2024).

(a) Alignment between multimodal supervision with the projected state and relation effect tokens.

AEM	$\mathcal{L}_s^{\text{eff}}$		$\mathcal{L}_r^{\text{eff}}$		AUC	EDA
	Visual	Textual	Visual	Textual		
X			N/A		67.6	65.6
✓	X	X	X	X	67.9	65.8
	✓	✓	X	X	68.4	66.1
	X	X	✓	✓	69.4	66.3
	✓	✓	✓	X	<u>71.7</u>	<u>66.4</u>
	X	✓	X	✓	69.9	66.0
	✓	✓	✓	✓	73.8	66.7

(d) Alignment of supervisions in state and relation spaces.

$\mathcal{L}_s^{\text{CL}}$	$\mathcal{L}_r^{\text{CL}}$	AUC	EDA
X	X	66.8	64.7
✓	X	69.9	64.5
X	✓	<u>72.6</u>	<u>65.1</u>
✓	✓	73.8	66.7

(f) Performance comparison of our method with different scene graph generation models.

Models	Quesadilla		Oatmeal		Pinwheel		Coffee		Tea		All	
	AUC	EDA	AUC	EDA	AUC	EDA	AUC	EDA	AUC	EDA	AUC	EDA
Qwen3-VL	77.8	69.0	77.3	68.8	70.0	62.2	70.2	64.3	71.4	68.7	73.3	66.6
GPT-4o	80.8	68.1	77.0	68.6	69.9	61.2	70.3	66.4	71.1	69.4	73.8	66.7

(b) Effect-frame sampling strategies.

Method	AUC	EDA
w/o Effect	67.6	65.6
Last Frame	<u>70.6</u>	<u>65.7</u>
Ours	73.8	66.7

(c) Dynamic cross-level interactions.

Method	AUC	EDA
AMNAR	68.5	<u>64.4</u>
w/o Dyn	<u>71.8</u>	63.4
w/ Dyn	73.8	66.7

(e) Action segmentation performance.

Method	IoU	Edit	F1@0.5	Acc
EgoPED	44.6	61.3	47.5	68.5
AMNAR	<u>56.3</u>	<u>69.4</u>	<u>57.3</u>	75.3
Ours	58.5	69.7	58.5	<u>73.5</u>

recipes as the final performance. Both the effect-frame sampling and multimodal knowledge extraction are performed during the *data pre-processing* stage to avoid additional training overhead. All experiments are conducted using an NVIDIA RTX 6000 Ada GPU (48GB memory).

4.2 COMPARISON WITH STATE-OF-THE-ART

We compare our methods with video anomaly detection methods HF²-VAD (Liu et al., 2021), HF²-VAD + SSPCAB (Ristea et al., 2022) and S3R (Wu et al., 2022), as well as mistake detection methods EgoPED (Lee et al., 2024) and AMNAR (Huang et al., 2025a). As shown in Table 1, on the EgoPER dataset, our method outperforms in both metrics on most of the five tasks, with an average improvement of 5.3% on AUC and 2.3% on EDA. The results in Table 2 further demonstrate its effectiveness on the CaptainCook4D dataset, surpassing AMNAR by 2.7% in Precision and 2.3% in AUC. On both datasets, our EDA is occasionally lower than that of AMNAR. This gap is likely due to AMNAR’s use of a dynamic programming block to construct task graphs that mitigate noise in action-segment labels. Since incorporating task graphs lies beyond the scope of our work, we leave it for future exploration.

4.3 ABLATION STUDIES

In the ablation study, we aim to answer the following questions:

1. Is Action Effect Modeling effective and generalizable?
2. Which is more important: object state effect or spatial relation effect?
3. How do visual and textual signals contribute to AEM?
4. Is aligning external multimodal features necessary?
5. How do different effect-frame sampling strategies perform?
6. Does multi-scale dynamic fusion module contribute to mistake detection?
7. Can open-source MLLMs replace the expensive closed-source models?

1) *Action Effect Modeling*. As shown in Table 3a, the first row reports the performance of baseline, which already achieves a comparable performance to AMNAR. This is attributed to the prompt-based detector’s ability to capture task-specific action representations, thereby enhancing the discriminability of action execution. The 2nd row further demonstrates that the learnable token can implicitly model action effects without relying on contextual knowledge provided by Grounding DINO or GPT-4o. After introducing different forms of external supervision, our model achieves consistent improvements, verifying its generalizability. Finally, when combining all multimodal effect supervision signals, our model achieves the best performance due to supervised effect modeling.

2) *State vs. Relation Effect*. The 3rd and 4th rows of Table 3a show the impact of state and relational effects. Compared to implicit token learning, explicitly introducing supervision signals for state or relational effects leads to performance gains, where relational supervision performs better, yielding a 1.0% improvement in AUC over state supervision. We argue that spatial relationships between objects provide more consistent and discriminative cues for action correctness. In contrast, object state changes are often subtle and visually ambiguous, making them more difficult to capture reliably.

3) *Visual vs. Textual Supervision*. The 5th and 6th rows of Table 3a report the impact of incorporating visual and textual features as external knowledge. Compared to baseline, using visual features improves AUC to 71.7% and EDA to 66.4%, while textual features yield a smaller gain. We argue that visual features are more effective because they directly capture object appearance and spatial layout, offering fine-grained cues to reflect execution-related visual differences. In contrast, textual features, although semantically informative, are abstracted from generated scene graphs and may introduce noise or miss subtle visual distinctions in complex egocentric environments.

4) *Effect Feature Alignment*. We further study the impact of aligning multimodal supervision features in state and relation effect representation spaces. As shown in Table 3d, using unaligned visual and textual supervisions leads to a suboptimal AUC of 66.8% and EDA of 64.7%, even lower than the model without effect modeling, highlighting the importance of cross-modal alignment. Introducing contrastive alignment in either the state space or the relation space improves AUC to 69.9% and 72.6%, improves EDA to 64.5% and 65.1%. The stronger gain from relation alignment suggests that object spatial relationships play a more critical role in modeling action effects. Finally, aligning both state and relation representations achieves the best AUC, demonstrating the complementary nature of these two effect types and the effectiveness of joint cross-modal supervision.

5) *Effect Frame Sampling*. To assess the effectiveness of our effect-frame sampling strategy, we compare it with a naive baseline that selects the last frame of each action segment, assuming that action effects are most visible at the end. As shown in Table 3b, this heuristic raises AUC to 70.6%, confirming that incorporating effect information benefits mistake detection. In contrast, our proposed strategy, which jointly considers semantic relevance and visual clarity further, boosts AUC to 73.8% and EDA to 66.7%. These results imply that a more informed selection of effect frames yields more discriminative representations, thereby improving detection performance.

6) *Dynamic Fusion Module*. Table 3c evaluates whether enhancing multi-scale temporal representations contributes to the final detection performance. Results show that incorporating the dynamic fusion yields a 2% improvement in AUC and a 3.3% gain in EDA, highlighting the importance of expressive action segment representations for downstream mistake detection. Notably, even without this module, our model still surpasses AMNAR by 3.3% AUC and achieves comparable EDA, further highlighting the superiority of our overall framework.

7) *Alternative open-source MLLM*. In this work, we employ GPT-4o (Hurst et al., 2024) to generate action scene graphs that provide supervision signals for our method. To assess whether alternative models can fulfill the same role, we replace GPT-4o with the open-source MLLM Qwen3-VL (30B) (Bai et al., 2025). As shown in Table 3f, scene graphs generated by Qwen3-VL yield mistake detection performance comparable to that with GPT-4o, indicating that open-source models can serve as a cost-effective alternative for scene graph generation while maintaining strong performance.

4.4 ACTION SEGMENTATION

Table 3e presents a comparison of action segmentation performance. All models, including ours, use ActionFormer (Zhang et al., 2022) as the segmentation backbone, ensuring a fair comparison. Our approach outperforms prior methods across most evaluation metrics, highlighting its effectiveness

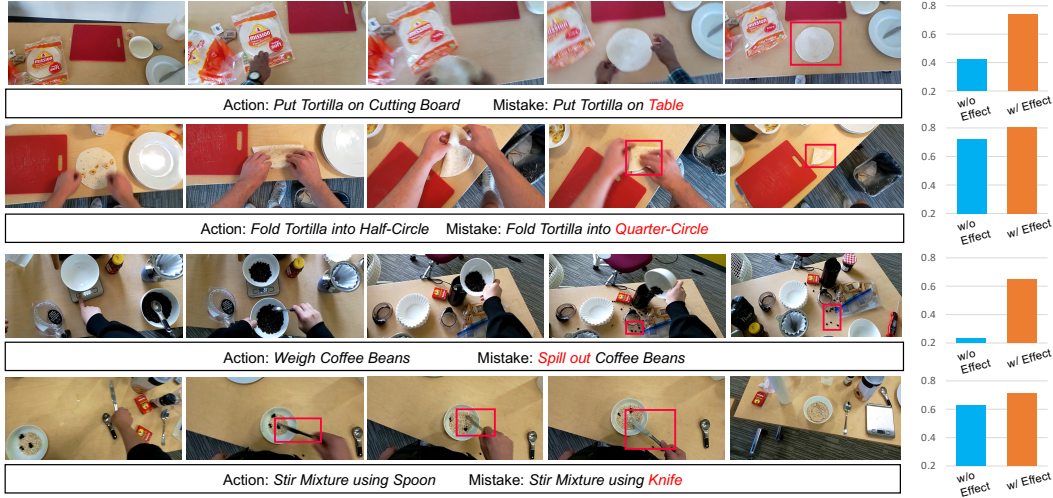


Figure 4: Examples of mistakes occurring in different actions. The right bar charts show mistake probabilities predicted by models without (in blue) and with (in orange) effect modeling. Red boxes in images are only used to highlight mistake regions for clearer visualization.

in enhancing action segmentation in addition to mistake detection. These results also indicate that our framework holds promise for broader video understanding tasks where action effects serve as critical cues, such as action recognition (Bao et al., 2021) and action analysis (Huang et al., 2025b).

4.5 QUALITATIVE ANALYSIS

Figure 4 shows visualizations of the action segments and their corresponding predicted mistake probabilities. The results highlight two key advantages of our approach: (i) the model effectively detects errors that appear in the final outcomes through action–effect modeling (row 1 to row 3), and (ii) it can also identify execution errors that arise during the process enabled by the prompt-based detector, even when the visual outcome seems correct (row 4). Together, these findings demonstrate the complementarity between effect-aware representations and temporal execution modeling in capturing a broader spectrum of procedural errors.

5 CONCLUSION

We presented a unified framework for procedural mistake detection that explicitly models the relationship between action execution and its resulting effect. The proposed Action Effect Modeling (AEM) enriches action representations with effect-aware cues by integrating object states and spatial relationships, guided through multimodal supervision. Combined with a prompt-based detector, our framework effectively captures both subtle execution errors and outcome discrepancies, achieving substantial improvements over prior methods on mistake detection benchmarks. Future work could extend the approach to multi-step reasoning for more comprehensive procedural activity understanding and mistake detection.

REFERENCES

- Anas Al-Lahham, Nurbek Tastan, Muhammad Zaigham Zaheer, and Karthik Nandakumar. A coarse-to-fine pseudo-labeling (c2fpl) framework for unsupervised video anomaly detection. In *Proceedings of the IEEE/CVF Winter Conference on Applications of Computer Vision*, pp. 6793–6802, 2024.
- Kumar Ashutosh, Santhosh Kumar Ramakrishnan, Triantafyllos Afouras, and Kristen Grauman. Video-mined task graphs for keystone recognition in instructional videos. *Advances in Neural Information Processing Systems*, 36, 2024.

- Shuai Bai, Yuxuan Cai, Ruizhe Chen, Keqin Chen, Xionghui Chen, Zesen Cheng, Lianghao Deng, Wei Ding, Chang Gao, Chunjiang Ge, Wenbin Ge, Zhifang Guo, Qidong Huang, Jie Huang, Fei Huang, Binyuan Hui, Shutong Jiang, Zhaohai Li, Mingsheng Li, Mei Li, Kaixin Li, Zicheng Lin, Junyang Lin, Xuejing Liu, Jiawei Liu, Chenglong Liu, Yang Liu, Dayiheng Liu, Shixuan Liu, Dunjie Lu, Ruilin Luo, Chenxu Lv, Rui Men, Lingchen Meng, Xuancheng Ren, Xingzhang Ren, Sibao Song, Yuchong Sun, Jun Tang, Jianhong Tu, Jianqiang Wan, Peng Wang, Pengfei Wang, Qiuyue Wang, Yuxuan Wang, Tianbao Xie, Yiheng Xu, Haiyang Xu, Jin Xu, Zhibo Yang, Mingkun Yang, Jianxin Yang, An Yang, Bowen Yu, Fei Zhang, Hang Zhang, Xi Zhang, Bo Zheng, Humen Zhong, Jingren Zhou, Fan Zhou, Jing Zhou, Yuanzhi Zhu, and Ke Zhu. Qwen3-vl technical report. *arXiv preprint arXiv:2511.21631*, 2025.
- Wentao Bao, Qi Yu, and Yu Kong. Evidential deep learning for open set action recognition. In *Proceedings of the IEEE/CVF international conference on computer vision*, pp. 13349–13358, 2021.
- Guodong Ding, Fadime Sener, Shugao Ma, and Angela Yao. Every mistake counts in assembly. *arXiv preprint arXiv:2307.16453*, 2023.
- Yuxin Fang, Quan Sun, Xinggang Wang, Tiejun Huang, Xinlong Wang, and Yue Cao. Eva-02: A visual representation for neon genesis. *Image and Vision Computing*, pp. 105171, 2024.
- Alessandro Flaborea, Guido Maria D’Amely di Melendugno, Leonardo Plini, Luca Scofano, Edoardo De Matteis, Antonino Furnari, Giovanni Maria Farinella, and Fabio Galasso. Prego: online mistake detection in procedural egocentric videos. In *Proceedings of the IEEE/CVF Conference on Computer Vision and Pattern Recognition*, pp. 18483–18492, 2024.
- Reza Ghoddoosian, Isht Dwivedi, Nakul Agarwal, and Behzad Dariush. Weakly-supervised action segmentation and unseen error detection in anomalous instructional videos. In *Proceedings of the IEEE/CVF International Conference on Computer Vision*, pp. 10128–10138, 2023.
- Dong Gong, Lingqiao Liu, Vuong Le, Budhaditya Saha, Moussa Reda Mansour, Svetha Venkatesh, and Anton van den Hengel. Memorizing normality to detect anomaly: Memory-augmented deep autoencoder for unsupervised anomaly detection. In *Proceedings of the IEEE/CVF international conference on computer vision*, pp. 1705–1714, 2019.
- Yuto Haneji, Taichi Nishimura, Hirotaka Kameko, Keisuke Shirai, Tomoya Yoshida, Keiya Kajimura, Koki Yamamoto, Taiyu Cui, Tomohiro Nishimoto, and Shinsuke Mori. Egooops: A dataset for mistake action detection from egocentric videos with procedural texts. *arXiv preprint arXiv:2410.05343*, 2024.
- Wei-Jin Huang, Yuan-Ming Li, Zhi-Wei Xia, Yu-Ming Tang, Kun-Yu Lin, Jian-Fang Hu, and Wei-Shi Zheng. Modeling multiple normal action representations for error detection in procedural tasks. In *Proceedings of the Computer Vision and Pattern Recognition Conference*, pp. 27794–27804, 2025a.
- Zhanbo Huang, Xiaoming Liu, and Yu Kong. H-more: Learning human-centric motion representation for action analysis. In *Proceedings of the Computer Vision and Pattern Recognition Conference*, pp. 22702–22713, 2025b.
- Aaron Hurst, Adam Lerer, Adam P Goucher, Adam Perelman, Aditya Ramesh, Aidan Clark, AJ Ostrow, Akila Welihinda, Alan Hayes, Alec Radford, et al. Gpt-4o system card. *arXiv preprint arXiv:2410.21276*, 2024.
- Youngkyoon Jang, Brian Sullivan, Casimir Ludwig, Iain Gilchrist, Dima Damen, and Walterio Mayol-Cuevas. Epic-tent: An egocentric video dataset for camping tent assembly. In *Proceedings of the IEEE/CVF International Conference on Computer Vision Workshops*, pp. 0–0, 2019.
- Yunseok Jang, Sungryull Sohn, Lajanugen Logeswaran, Tiange Luo, Moontae Lee, and Honglak Lee. Multimodal subtask graph generation from instructional videos. *arXiv preprint arXiv:2302.08672*, 2023.
- Shih-Po Lee, Zijia Lu, Zekun Zhang, Minh Hoai, and Ehsan Elhamifar. Error detection in egocentric procedural task videos. In *Proceedings of the IEEE/CVF Conference on Computer Vision and Pattern Recognition*, pp. 18655–18666, 2024.

- Shilong Liu, Zhaoyang Zeng, Tianhe Ren, Feng Li, Hao Zhang, Jie Yang, Qing Jiang, Chunyuan Li, Jianwei Yang, Hang Su, et al. Grounding dino: Marrying dino with grounded pre-training for open-set object detection. In *European Conference on Computer Vision*, pp. 38–55. Springer, 2024.
- Zhian Liu, Yongwei Nie, Chengjiang Long, Qing Zhang, and Guiqing Li. A hybrid video anomaly detection framework via memory-augmented flow reconstruction and flow-guided frame prediction. In *Proceedings of the IEEE/CVF international conference on computer vision*, pp. 13588–13597, 2021.
- Michele Mazzamuto, Antonino Furnari, and Giovanni Maria Farinella. Eyes wide unshut: Unsupervised mistake detection in egocentric video by detecting unpredictable gaze. *arXiv preprint arXiv:2406.08379*, 2024.
- Yue Meng, Chung-Ching Lin, Rameswar Panda, Prasanna Sattigeri, Leonid Karlinsky, Aude Oliva, Kate Saenko, and Rogerio Feris. Ar-net: Adaptive frame resolution for efficient action recognition. In *European conference on computer vision*, pp. 86–104. Springer, 2020.
- Medhini Narasimhan, Licheng Yu, Sean Bell, Ning Zhang, and Trevor Darrell. Learning and verification of task structure in instructional videos. *arXiv preprint arXiv:2303.13519*, 2023.
- Yulei Niu, Wenliang Guo, Long Chen, Xudong Lin, and Shih-Fu Chang. Schema: State changes matter for procedure planning in instructional videos. *arXiv preprint arXiv:2403.01599*, 2024.
- Rohith Peddi, Shivvrat Arya, Bharath Challa, Likhitha Pallapothula, Akshay Vyas, Jikai Wang, Qifan Zhang, Vasundhara Komaragiri, Eric Ragan, Nicholas Ruozzi, et al. Captaincook4d: A dataset for understanding errors in procedural activities. *arXiv preprint arXiv:2312.14556*, 2023.
- Leonardo Plini, Luca Scofano, Edoardo De Matteis, Guido Maria D’Amely di Melendugno, Alessandro Flaborea, Andrea Sanchietti, Giovanni Maria Farinella, Fabio Galasso, and Antonino Furnari. Ti-prego: Chain of thought and in-context learning for online mistake detection in procedural egocentric videos. *arXiv preprint arXiv:2411.02570*, 2024.
- Yujiang Pu and Xiaoyu Wu. Audio-guided attention network for weakly supervised violence detection. In *2022 2nd International Conference on Consumer Electronics and Computer Engineering (ICCECE)*, pp. 219–223. IEEE, 2022.
- Yujiang Pu, Xiaoyu Wu, Lulu Yang, and Shengjin Wang. Learning prompt-enhanced context features for weakly-supervised video anomaly detection. *IEEE Transactions on Image Processing*, 2024.
- Nicolae-Cătălin Ristea, Neelu Madan, Radu Tudor Ionescu, Kamal Nasrollahi, Fahad Shahbaz Khan, Thomas B Moeslund, and Mubarak Shah. Self-supervised predictive convolutional attentive block for anomaly detection. In *Proceedings of the IEEE/CVF conference on computer vision and pattern recognition*, pp. 13576–13586, 2022.
- Tim J Schoonbeek, Tim Houben, Hans Onvlee, Fons Van der Sommen, et al. Industreal: A dataset for procedure step recognition handling execution errors in egocentric videos in an industrial-like setting. In *Proceedings of the IEEE/CVF Winter Conference on Applications of Computer Vision*, pp. 4365–4374, 2024.
- Fadime Sener, Dibyadip Chatterjee, Daniel Shelepov, Kun He, Dipika Singhania, Robert Wang, and Angela Yao. Assembly101: A large-scale multi-view video dataset for understanding procedural activities. In *Proceedings of the IEEE/CVF Conference on Computer Vision and Pattern Recognition*, pp. 21096–21106, 2022.
- Bilge Soran, Ali Farhadi, and Linda Shapiro. Generating notifications for missing actions: Don’t forget to turn the lights off! In *Proceedings of the IEEE International Conference on Computer Vision*, pp. 4669–4677, 2015.
- Shane Storks, Itamar Bar-Yossef, Yayuan Li, Zheyuan Zhang, Jason J Corso, and Joyce Chai. Explainable procedural mistake detection. *arXiv preprint arXiv:2412.11927*, 2024.

- Petar Veličković, Guillem Cucurull, Arantxa Casanova, Adriana Romero, Pietro Lio, and Yoshua Bengio. Graph attention networks. *arXiv preprint arXiv:1710.10903*, 2017.
- Xin Wang, Taein Kwon, Mahdi Rad, Bowen Pan, Ishani Chakraborty, Sean Andrist, Dan Bohus, Ashley Feniello, Bugra Tekin, Felipe Vieira Frujeri, et al. Holoassist: an egocentric human interaction dataset for interactive ai assistants in the real world. In *Proceedings of the IEEE/CVF International Conference on Computer Vision*, pp. 20270–20281, 2023.
- Jhih-Ciang Wu, He-Yen Hsieh, Ding-Jie Chen, Chiou-Shann Fuh, and Tyng-Luh Liu. Self-supervised sparse representation for video anomaly detection. In *European Conference on Computer Vision*, pp. 729–745. Springer, 2022.
- Peng Wu, Jing Liu, and Fang Shen. A deep one-class neural network for anomalous event detection in complex scenes. *IEEE transactions on neural networks and learning systems*, 31(7):2609–2622, 2019.
- Le Yang, Ziwei Zheng, Yizeng Han, Hao Cheng, Shiji Song, Gao Huang, and Fan Li. Dyfadet: Dynamic feature aggregation for temporal action detection. In *European Conference on Computer Vision (ECCV)*, 2024.
- Chen-Lin Zhang, Jianxin Wu, and Yin Li. Actionformer: Localizing moments of actions with transformers. In *European Conference on Computer Vision*, pp. 492–510. Springer, 2022.